



# Enhanced adsorption of phosphate from aqueous solution by nanostructured iron(III)–copper(II) binary oxides

Guoliang Li<sup>a,b</sup>, Song Gao<sup>c</sup>, Gaosheng Zhang<sup>a,b,\*</sup>, Xiwang Zhang<sup>d</sup>

<sup>a</sup>Key Laboratory of Coastal Zone Environmental Processes, Yantai Institute of Coastal Zone Research (YIC), Chinese Academy of Sciences (CAS), 17th Chunhui Road, Yantai, Shandong 264003, China

<sup>b</sup>Shandong Provincial Key Laboratory of Coastal Zone Environmental Processes, YICCAS, 17th Chunhui Road, Yantai, Shandong 264003, China

<sup>c</sup>Environment and Material Engineering College, Yantai University, 32th Qingquan Road, Yantai 264005, China

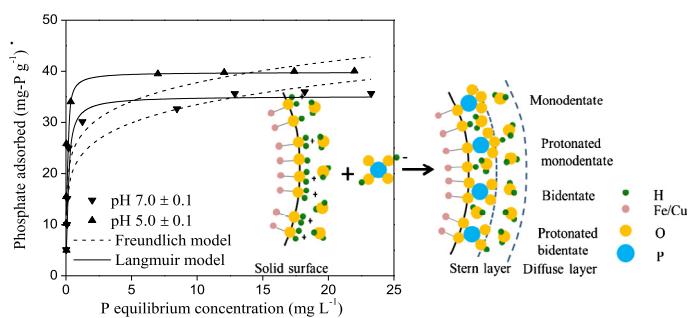
<sup>d</sup>School of Applied Sciences and Engineering, Monash University Gippsland Campus, Churchill, Vic 3842, Australia

## HIGHLIGHTS

- The Fe–Cu binary oxide was effective for phosphate removal from water.
- Phosphate was removed via replacing the surface sulfate and hydroxyl groups.
- It could be effectively regenerated with dilute NaOH solution.

## GRAPHICAL ABSTRACT

Adsorption isotherms and mechanism of phosphate by Fe–Cu binary oxide, which demonstrate high phosphate adsorption capacity and the possible adsorption process.



## ARTICLE INFO

### Article history:

Received 15 April 2013

Received in revised form 18 August 2013

Accepted 4 September 2013

Available online 12 September 2013

### Keywords:

Fe–Cu binary oxide  
Phosphate  
Adsorption  
Mechanism

## ABSTRACT

Phosphate is one of the main elements causing eutrophication and hence the development of high-efficiency and low-cost technologies for phosphate removal from water is of vital importance to alleviate the situation. In this study, nanostructured Fe–Cu binary oxides were synthesized via a facile coprecipitation process and its performance on phosphate removal was systematically evaluated. The as-prepared adsorbent with a Cu/Fe molar ratio of 1:2 was proved to possess the highest phosphate adsorption capacity. The adsorption isotherm data gave better fit to the Langmuir model, with a maximum phosphate adsorption capacity of  $35.2 \text{ mg g}^{-1}$  at  $\text{pH } 7.0 \pm 0.1$ . Kinetic data correlated well with the pseudo-second-order kinetic model, indicating that the adsorption process might be chemical sorption. Thermodynamic data validated that the phosphate adsorption was an endothermic process. The solution pH has a big impact on the phosphate adsorption on the sorbent and acidic condition was favorable for the adsorption. The coexisting  $\text{Cl}^-$ ,  $\text{SO}_4^{2-}$  and  $\text{HCO}_3^-$  anions had no significant influence on phosphate adsorption, while the present  $\text{F}^-$  and  $\text{SiO}_3^{2-}$  could suppress its adsorption, especially at high concentration level. The phosphate adsorption might be mainly achieved by the replacement of surface sulfate and hydroxyl groups by the phosphate species and formation of inner-sphere surface complexes at the water/oxide interface. Moreover, the spent Fe–Cu binary oxide could be effectively regenerated by NaOH solution for reuse. The high phosphate uptake capability and good reusability of the Fe–Cu binary oxide make it a potentially attractive adsorbent for the removal of phosphate from water.

© 2013 Elsevier B.V. All rights reserved.

\* Corresponding author at. Key Laboratory of Coastal Zone Environmental Processes, Yantai Institute of Coastal Zone Research (YIC), Chinese Academy of Sciences (CAS), 17th Chunhui Road, Yantai, Shandong 264003, China. Tel.: +86 0535 2109139.

E-mail addresses: [gszhang@yic.ac.cn](mailto:gszhang@yic.ac.cn), [zgs77@126.com](mailto:zgs77@126.com) (G. Zhang).

## 1. Introduction

Phosphate is an essential macronutrient that is critically needed for biomass growth and the normal functioning of ecosystems [1,2]. However, an excessive intake of phosphate in water bodies may spur an abnormal growth of algae and aquatic plants [1], which poses a risk of eutrophication to the receiving water bodies. It is believed that once the concentration of phosphate in lakes or sea is over  $0.03 \text{ mg L}^{-1}$ , algae bloom or red tide will occur [3]. Therefore, phosphate removal is critically necessary for phosphate-bearing wastewater prior to its discharge into the water environment [4].

Several methods have been used to remove phosphate from wastewater, such as chemical precipitation [5], biological processes [6], adsorption [7], ion exchange [8], membrane technologies [9] and constructed wetlands [10]. Among these available approaches, adsorption method is believed to be one of the most economical, effective, and reliable methods. Another attractive feature of this technique is that the nutrient-loaded filters can be used in agriculture as phosphate fertilizer and soil conditioner [11]. Various materials, including natural minerals, industrial by-products (fly ash, steel slag and red mud) and synthetic adsorbents, have been used to remove phosphate from wastewater [12–15]. Among them, iron (hydr)oxides, including amorphous hydrous ferric oxide, poorly crystalline hydrous ferric oxide (ferrihydrite) [16], goethite and akaganeite [17], are well-known due to their high affinity toward phosphate, low cost, and environmental friendliness.

In recent years, the development of composite adsorbents containing two (or more) different metal oxides for phosphate removal has gained increasing attention. For instances, Al–Fe hydr(oxides) [18], Fe–Mn binary oxide [19], Fe–Zr binary oxide [20], mesoporous spheres containing iron and aluminum oxide [21], hydroxyl-iron-lanthanum doped activated carbon fiber [22] and Fe–Al–Mn trimetal oxide [23] have been reported for phosphate removal. The composite adsorbents possess superior adsorption performance since they inherit the advantages of their parent materials.

In our previous studies [24] a novel nanostructured Fe(III)–Cu(II) binary oxide was successfully synthesized, aiming at enhancing arsenic sorption performance. It was found that the prepared binary oxide was excellent sorbent for both arsenate and arsenite removal, but the present phosphate anions competed strongly with arsenic for sorption sites on surface of the binary oxide. Hence, we anticipated that the Fe–Cu binary oxide would have promising potential to be used as adsorbent for phosphate removal. However, up to now, no systematic investigation of phosphate adsorption by Fe–Cu binary oxide has been reported.

Therefore, a series of Fe–Cu binary oxides with different Cu/Fe molar ratios (from 0:1 to 1:0) were prepared and were tested for phosphate adsorption in this study. The adsorption kinetics, adsorption isotherms, regeneration and reusability as well as the influences of solution pH, ionic strength and coexisting anions on phosphate adsorption were investigated. Moreover, phosphate adsorption mechanism was elucidated in the present paper. The results would provide a new insights on the development of high performance sorbent for phosphate removal.

## 2. Materials and methods

### 2.1. Materials

Anhydrous potassium dihydrogen orthophosphate ( $\text{KH}_2\text{PO}_4$ ) are guaranteed grade and other reagents all are analytical grade. All chemicals were used as without further purification. Reaction vessels (glass) were cleaned with 1%  $\text{HNO}_3$  and rinsed several times with deionized water before use. Phosphate stock solution was

prepared by dissolving appropriate amounts of  $\text{KH}_2\text{PO}_4$  in deionized water, and the working solutions were freshly prepared by diluting phosphate stock with deionized water.

### 2.2. Preparation of Fe–Cu binary oxides

A series of Fe–Cu binary oxides were synthesized at different Cu:Fe molar ratios, 0:1, 1:10, 1:5, 1:3, 1:2, 1:1.5, 1:1 and 1:0, respectively. Typically, predetermined amount of ferric chloride hexahydrate ( $\text{FeCl}_3 \cdot 6\text{H}_2\text{O}$ ) and copper(II) sulfate pentahydrate ( $\text{CuSO}_4 \cdot 5\text{H}_2\text{O}$ ) were dissolved in 400 ml deionized water. Under vigorous magnetic-stirring, sodium hydroxide solution ( $3 \text{ mol L}^{-1}$ ) was added dropwise to raise the solution pH to 7.5. The formed suspension was continuously stirred for 1 h and aged at room temperature for 4 h. After washing several times with deionized water, the suspension was then filtrated and dried at  $55^\circ\text{C}$  for 24 h. Subsequently, the dry material was ground into fine powder and stored in a desiccator for use.

### 2.3. Adsorption experiments

#### 2.3.1. Influence of Cu/Fe molar ratio on phosphate adsorption

To determine the optimal Cu:Fe molar ratio, batch tests were carried out to compare the adsorption capacity of Fe–Cu binary oxides of different Cu:Fe molar ratio. Glass vessels with a volume of 150 ml, containing 50 ml of  $7.0 \text{ mg L}^{-1}$  phosphate solution, were used. The sorbent dosage was  $10 \text{ mg L}^{-1}$ . The vessels were shaken on an orbit shaker at 160 rpm for 24 h at  $25 \pm 1^\circ\text{C}$  to reach adsorption equilibrium. The pH of the solutions was adjusted every four hours with dilute  $\text{HNO}_3$  or/and  $\text{NaOH}$  solution to  $\text{pH } 7.0 \pm 0.1$  during adsorption process. After the adsorption of 24 h, the mixture was filtered through a  $0.45 \mu\text{m}$  membrane. Then, the residual phosphate concentration and pH in the supernatant solutions were measured.

#### 2.3.2. Adsorption kinetics

The kinetics experiments were carried out at  $25 \pm 1^\circ\text{C}$  using 1000 ml of  $5.0 \text{ mg L}^{-1}$  phosphate solution. The ionic strength was maintained at  $0.01 \text{ mol L}^{-1}$  by adding an appropriate amount of  $\text{NaNO}_3$ . After the solution pH was adjusted to  $7.0 \pm 0.1$  by adding  $0.1 \text{ mol L}^{-1}$   $\text{HNO}_3$  and/or  $\text{NaOH}$ ,  $0.2 \text{ g}$  Fe–Cu binary oxide was added to obtain a  $0.2 \text{ g L}^{-1}$  suspension. The suspension was mixed with a magnetic stirrer at 160 rpm. Samples of 5 ml were taken from the suspension at predetermined times. The samples were immediately filtered through a  $0.45 \mu\text{m}$  membrane filter and residual phosphate concentrations in filtrates were determined. The adsorbent powders were taken out for further characterization.

#### 2.3.3. Adsorption isotherms

The adsorption isotherms were determined using batch tests at respective pH,  $5.0 \pm 0.1$  and  $7.0 \pm 0.1$ . The pH of suspensions was adjusted with 0.1 M of  $\text{NaOH}$  and  $\text{HNO}_3$  during the experiments. Initial phosphate concentration varied from 1 to  $30 \text{ mg L}^{-1}$ . In each test, 10 mg adsorbent was loaded in a 150-ml glass vessel containing 50 ml phosphate solution of predetermined concentration. Ionic strength of the solution was adjusted to  $0.01 \text{ mol L}^{-1}$  with  $\text{NaNO}_3$ . The vessels were shaken on an orbit shaker at 160 rpm for 24 h at  $25 \pm 1^\circ\text{C}$ . Furthermore, in order to study the influence of temperature on phosphate adsorption, batch tests were also conducted at other two temperatures of  $15 \pm 1^\circ\text{C}$  and  $35 \pm 1^\circ\text{C}$ .

#### 2.3.4. Effect of pH and ionic strength

To investigate the influence of pH and ionic strength on the phosphate adsorption, experiments were carried out using 150 ml glass vessels containing 50 ml phosphate solution. The phosphate concentration was of  $5.2 \text{ mg L}^{-1}$  and the sorbent dosage

was 0.2 g L<sup>-1</sup>. The ionic strength of the solutions varied from 0.001 to 0.1 mol L<sup>-1</sup> by adding different amounts of NaNO<sub>3</sub>. The pH of the solutions were adjusted every 2 h with dilute HCl and/or NaOH solution to designated values.

### 2.3.5. Effect of coexisting anions

The effect of common coexisting ions in wastewater such as Cl<sup>-</sup>, F<sup>-</sup>, HCO<sub>3</sub><sup>-</sup>, SO<sub>4</sub><sup>2-</sup> and SiO<sub>3</sub><sup>2-</sup> on the phosphate adsorption were investigated by adding NaCl, NaF, NaHCO<sub>3</sub>, K<sub>2</sub>SO<sub>4</sub>, NaSiO<sub>3</sub> to 5 mg L<sup>-1</sup> of phosphate solution, respectively. The anion concentrations ranged from 5 to 100 mg L<sup>-1</sup>. The solution pH was adjusted to 7.0 ± 0.1. 10 mg of Fe–Cu binary oxide was added in each of the vessel containing 50 ml phosphate solution of 5 mg L<sup>-1</sup> and the solutions were mixed at 160 rpm for 24 h at 25 ± 1 °C. After filtration by a 0.45 μm membrane filter, the residual concentration of phosphate in the filtrates was analyzed.

### 2.3.6. Regeneration and reusability of the Fe–Cu binary oxide

Four cycles of adsorption and desorption were carried out to evaluate the reusability of the Fe–Cu binary oxide. For the adsorption tests, 400 mg of Fe–Cu sorbent was introduced into 1 L phosphate solution of 23 mg L<sup>-1</sup>. The solution was stirred continuously for 24 h at 160 rpm and 25 ± 1 °C. The pH of the solution was maintained at 7.0 ± 0.1 during adsorption process. Then the sorbents were separated by filtration and was used for desorption tests after drying at 55 °C for 1 d. For the desorption tests, the phosphate-containing Fe–Cu binary oxides were added into 100 ml NaOH solution of 0.5 mol L<sup>-1</sup>. The mixture was stirred for 6 h and then separated from the NaOH solution. After washing and drying, the sorbents were to be used in the next adsorption–desorption cycle.

### 2.4. Characterization before and after phosphate adsorption

The particle shapes and surface elements of prepared Fe–Cu binary oxide before and after phosphate adsorption were observed using a scanning electron microscope (SEM) with an EDAX (Hitachi S-4800). FTIR spectra were collected on a Nicolet IS10 FTIR spectrophotometer (Thermo scientific, USA) using a transmission model. Samples for FTIR determination were prepared via grinding 1 mg of sorbents with 80 mg of spectral grade KBr in an agate mortar. All IR measurements were carried out at room temperature.

### 2.5. Analytical methods

Phosphate was determined using an inductively coupled plasma atomic emission spectroscopy machine (ICP-OES, Optima 7100 DV, Perkin Elmer Co. USA). Prior to analysis, the aqueous samples were acidified with concentrated HCl in an amount of 1%, and stored in acid-washed glass vessels. All samples were analyzed within 24 h after collection.

## 3. Results and discussion

### 3.1. Influence of Cu:Fe molar ratio on phosphate sorption

To examine the effect of Cu:Fe molar ratio on phosphate adsorption, a serial of Fe–Cu binary oxides with different Cu:Fe molar ratios from 0:1 to 1:0, were synthesized. The oxides with molar ratios of 0:1 and 1:0 were known as FeOOH and CuO, respectively. Their morphologies and structures were observed by a scanning electron microscope and the images were shown in Fig. S1 (Supplementary materials). It can be found that the pure FeOOH grains were aggregates formed closely by ball-like nanoparticles, while the pure CuO grains were aggregates of pellet-like nanoparticles. With an increase Cu/Fe ratio, the grain size of Fe–Cu binary

oxide decreased and the structure was loosened. With the further increase in Cu/Fe ratio, the morphology and structure of Fe–Cu binary oxide were much more like those of pure CuO. Their adsorption capacities for phosphate removal were evaluated and the results are shown in Fig. 1. The adsorption capacity of phosphate on pure FeOOH is 12.6 mg g<sup>-1</sup>. It can be clearly seen from Fig. 1 that phosphate adsorption increased with an increase in Cu:Fe molar ratio and reached 31 mg g<sup>-1</sup> for the ratio of 1:2. Then, it dropped sharply with further increase in Cu:Fe molar ratio. For the pure CuO, it had a very low phosphate capacity of 3.9 mg g<sup>-1</sup>. This indicates that the introduction of copper oxide into iron oxide improved obviously the phosphate adsorption capacity. The looser structure of Fe–Cu binary oxide might result in a much higher specific surface area and porosity, which would facilitate the phosphate adsorption. However, an excessive CuO content in the binary oxide is not beneficial to phosphate uptake, which might be attributed to the low phosphate adsorption ability of copper oxide alone. Therefore, it can be concluded that the Cu:Fe molar ratio is a key factor influencing the adsorption capacity of the Fe–Cu binary oxide. The Fe–Cu binary oxide with the Cu:Fe molar ratio of 1:2 was used in the following experiments.

### 3.2. Adsorption kinetics

Kinetic experiments were performed to determine the adsorption rate of phosphate on the Fe–Cu oxide sorbent. The change of adsorbed phosphate as a function of adsorption time is shown in Fig. 2. It was found that the adsorption process could be divided into two steps, a quick step and a slow one. In the first step, the adsorption was very fast and appropriate 95% of the equilibrium adsorption capacity was achieved within the first 1 h. In the second step, the adsorption slowed down. Over 99.6% of the maximum adsorption had taken place within 16 h. To ensure complete adsorption, the adsorption time was therefore extended to 24 h for all batch experiments.

In order to evaluate the kinetic mechanism that control the adsorption process, Langergren pseudo-first-order model (Eq. (1)) and pseudo-second-order model (Eq. (2)) were employed to analyze the experimental data. Kinetic constants obtained from these two models are listed in Table 1.

$$\frac{dq_t}{dt} = k_1(q_e - q_t) \quad (1)$$

$$q_t = \frac{k_2 q_e^2 t}{1 + k_2 q_e t} \quad (2)$$

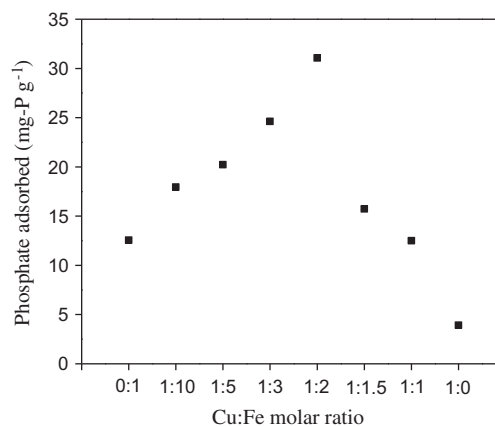
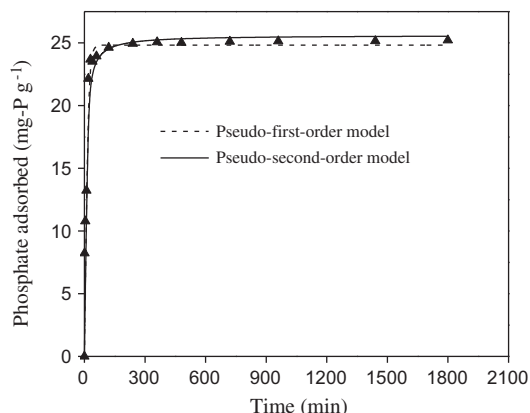


Fig. 1. Effect of Cu:Fe molar ratio on phosphate adsorption by Fe–Cu binary oxide. Initial phosphate concentration: 7.0 mg L<sup>-1</sup>, adsorbent dose: 200 mg L<sup>-1</sup>, pH: 7.0 ± 0.1, agitation speed: 160 rpm, and temperature: 25 ± 1 °C.



**Fig. 2.** Adsorption kinetics of phosphate on Fe–Cu binary oxide. Initial phosphate concentration: 5 mg L<sup>-1</sup>, adsorbent dose: 200 mg L<sup>-1</sup>, pH: 7.0 ± 0.1; agitation speed: 160 rpm, and temperature: 25 ± 1 °C.

where  $q_e$  and  $q_t$  are the adsorption capacities (mg g<sup>-1</sup>) of the adsorbent at equilibrium and at time  $t$  (min), respectively;  $k_1$  (min<sup>-1</sup>) and  $k_2$  (g mg<sup>-1</sup> min<sup>-1</sup>) are the related adsorption rate constants.

It is found that the kinetic data fitted better with the pseudo-second-order model, which is evident from the relatively higher correlation coefficient value ( $R^2 = 0.952$ ). This indicates that the adsorption process might be chemisorption [19].

### 3.3. Effect of pH and ionic strength

The effects of pH and ionic strength on the adsorption of phosphate were studied and the results were shown in Fig. 3. The adsorption capacity of the binary oxide was high in acidic condition while decreased with the increasing of solution pH in basic condition. Similar phenomena had been observed by other researchers in the studies of phosphate adsorption by iron or iron-based oxides [19,25]. Within the pH range of 3–11, negatively charged H<sub>2</sub>PO<sub>4</sub><sup>-</sup> and HPO<sub>4</sub><sup>2-</sup> are the dominated species of phosphate. On the one hand, ligand exchange might be the main adsorption mechanism for phosphate on synthesized Fe–Cu binary oxide, which releases OH<sup>-</sup> is more favorable at lower pH. On the other hand, low pH is beneficial for the surface protonation of the metal oxide. Increased protonation would increase the positively charged sites, enlarging the attraction force existing between the metal oxide surface and the negatively charged anions. Hence, higher adsorption capacity of phosphate on the sorbent was observed in the low pH region. In alkaline conditions, the negatively charged sites on the surface of metal oxide became dominated and the negatively charged phosphate species increased, which resulted in the repulsion between the phosphate ions and the binary oxide. As a result, phosphate adsorption dropped remarkably.

No significant change was found on phosphate adsorption as the ionic strength increased from 0.001 to 0.1 mol L<sup>-1</sup>. It is well known that anions adsorbed by outer-sphere association are strongly sensitive to ionic strength. The adsorption of these anions is hindered by competition with weakly adsorbing anions such as NO<sub>3</sub><sup>-</sup> since they also form outer-sphere complexes through electrostatic forces. On the contrary, anions adsorbed by inner-sphere

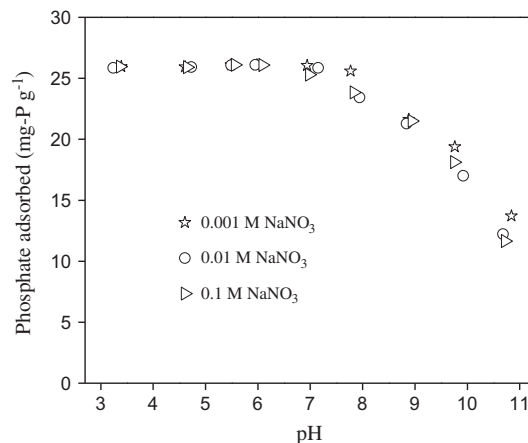


**Fig. 3.** Effects of solution pH and ionic strength on phosphate adsorption by Fe–Cu binary oxide. Initial phosphate concentration: 5.2 mg L<sup>-1</sup>, adsorbent dose: 200 mg L<sup>-1</sup>, agitation speed: 160 rpm, and temperature: 25 ± 1 °C.

association either show little sensitivity to ionic strength or respond to higher ionic strength with greater adsorption [26]. Based on this, it can be concluded that phosphate anions may be specifically adsorbed on the Fe–Cu binary oxide via forming inner-sphere surface complexes.

### 3.4. Adsorption isotherms

Batch isotherm studies were carried out to determine the maximum adsorption capacity of phosphate on Fe–Cu binary oxide. Fig. 4a shows the plots of the uptake of phosphate by the adsorbent against the phosphate equilibrium concentration in the solution at pH 5.0 ± 0.1 and pH 7.0 ± 0.1, respectively. Both Langmuir (Eq. (3)) and Freundlich (Eq. (4)) equations were employed to describe the adsorption isotherms data and the adsorption constants are listed in Table 2. The two equations can be expressed as follows:

$$\text{Langmuir equation : } q_e = q_{\max} \frac{K_L C_e}{1 + K_L C_e} \quad (3)$$

$$\text{Freundlich equation : } q_e = K_F C_e^n \quad (4)$$

where  $q_e$  and  $q_{\max}$  represent the amount of equilibrium adsorption capacity and the maximum adsorption capacity (mg g<sup>-1</sup>), respectively;  $C_e$  is the equilibrium solution concentration (mg L<sup>-1</sup>);  $K_L$  (L mg<sup>-1</sup>) is the Langmuir coefficient;  $K_F$  is roughly an indicator of the adsorption capacity and  $n$  is an empirical parameter.

Evidently, the oxide has a higher adsorption capacity at a lower pH value, which is in agreement with the result of solution pH effect on adsorption. As shown in Table 2, higher regression coefficient suggests that the Langmuir model is more suitable than Freundlich model at the two pH levels for describing the sorption behavior of phosphate on Fe–Cu binary oxide. The calculated maximal adsorption capacities for phosphate are 39.8 mg g<sup>-1</sup> at pH 5.0 ± 0.1 and 35.2 mg g<sup>-1</sup> at pH 7.0 ± 0.1, respectively. Compared to the adsorption capacities of other sorbents reported in the literature (Table 3), the Fe–Cu binary oxide sorbent possesses superior adsorption capacity. It is worth to note that the high adsorption

**Table 1**

Adsorption rate constants obtained from pseudo-first-order model and pseudo-second-order model.

Initial phosphate concentration (mg L <sup>-1</sup> )	Pseudo-first-order model			Pseudo-second-order model		
	$q_e$ (mg g <sup>-1</sup> )	$k_1$ (min <sup>-1</sup> )	$R^2$	$q_e$ (mg g <sup>-1</sup> )	$k_2$ (g/mg min)	$R^2$
5.0	24.8	0.101	0.948	25.6	0.007	0.952

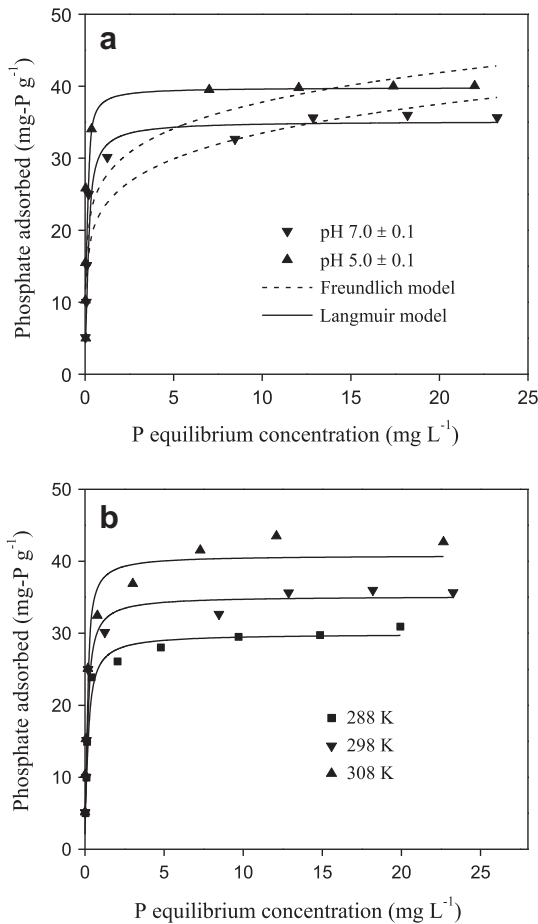


**Fig. 4.** Adsorption isotherms of phosphate by Fe–Cu binary oxide (a) at two pHs and  $T = 298$  K, and (b) at three different temperatures and at  $\text{pH } 7.0 \pm 0.1$ . (---) Freundlich model and (—) Langmuir model.

capacity of the binary oxide was achieved at a low equilibrium concentration ( $0.20 \text{ mg L}^{-1}$ ). Therefore, it might be more feasible for the removal of low concentration phosphate.

Additionally, the effect of three different temperatures (288, 298, and 308 K) on phosphate adsorption was examined at  $\text{pH } 7.0 \pm 0.1$  and the results were presented in Fig. 4b. The adsorption

**Table 2**  
Langmuir and Freundlich isotherm parameters for phosphate adsorption on Cu–Fe binary oxide at two pHs.

pH Value	Langmuir model			Freundlich model		
	$q_m$ ( $\text{mg g}^{-1}$ )	$K_L$ ( $\text{L mg}^{-1}$ )	$R^2$	$K_f$ ( $\text{mg g}^{-1}$ )	$n$	$R^2$
$5.0 \pm 0.1$	39.8	17.9	0.808	26.9	0.148	0.760
$7.0 \pm 0.1$	35.2	7.93	0.969	23.0	0.163	0.827

**Table 3**  
Comparison of maximum phosphate adsorption capacities for different adsorbents.

Adsorbents	Equilibrium Conc. ( $\text{mg L}^{-1}$ )	Solution pH	Max. adsorption capacity ( $\text{mg g}^{-1}$ )	Ref.
Fe–Cu binary oxide	0–25	7.0	35.2	Present study
Fe–Cu binary oxide	0–25	5.0	39.8	Present study
Blast furnace slags	0–400	7.0	18.9	[13]
Iron oxide tailings	0–140	6.6–6.8	8.2	[27]
Al oxide hydroxide	0–10	4	35	[3]
Mesoporous $\text{ZrO}_2$	0–275	6.7–6.9	29.7	[28]
La doped vesuvianite	0–4	7.1	6.7	[29]
Hydrous Nb oxide	0–22	2	15	[30]
Fe–Mn binary oxide	0–35	5.6	36	[19]
Magnetic Fe–Zr binary oxide	0–100	4.0	13.6	[20]

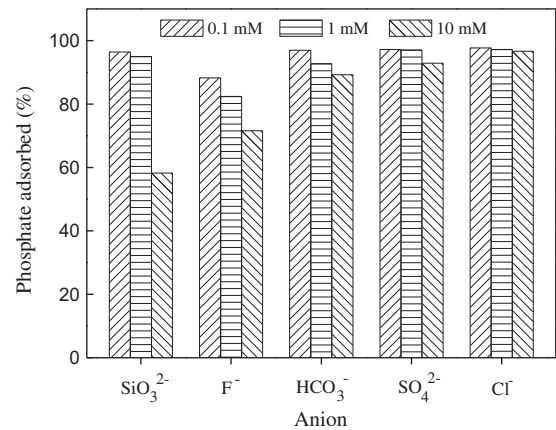


**Fig. 5.** Effect of co-existing anions on phosphate adsorption at fixed initial phosphate concentration:  $5 \text{ mg L}^{-1}$ , adsorbent dose:  $200 \text{ mg L}^{-1}$ ,  $\text{pH}: 7.0 \pm 0.1$ , agitation speed:  $160 \text{ rpm}$ , temperature:  $25 \pm 1$  °C.

isotherms at the three temperatures all were fitted very well by Langmuir model. It is found that the adsorption capacity increases with increasing temperature, which indicates that the adsorption process is endothermic in nature.

### 3.5. Effect of coexisting anions

Adsorption selectivity is an important factor influencing removal effectiveness. Some researchers employed highly selective adsorbents to separate or remove heavy metals from aqueous systems [31–33]. Anions such as bicarbonate, chloride, fluoride, sulfate, and silicate commonly exist in water or wastewater, and might interfere in the adsorption of phosphate through competing sorptive sites on the surface of the adsorbents. The effects of these anions on the phosphate adsorption at three concentration levels (0.1, 1.0, and 10 mM) were assessed at  $\text{pH } 7.0 \pm 0.1$  and the results are shown in Fig. 5.

For chloride, no obvious decrease in phosphate adsorption was observed when its concentration increased from 0.1 to 10 mM. For bicarbonate and sulfate, only a slight decrease was observed with increasing of their concentrations. The results suggest that these three anions have no significant influence in phosphate adsorption. However, the coexisting silicate and fluoride suppressed the phos-

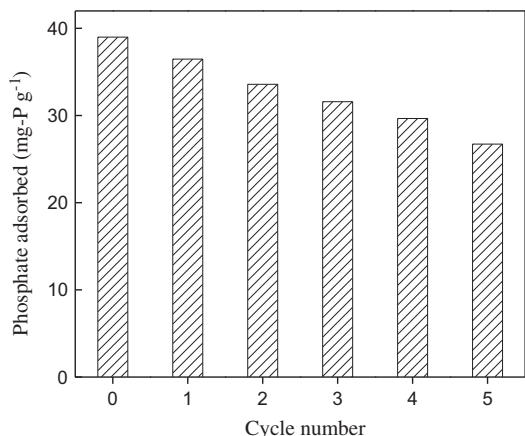


**Fig. 6.** Variation of the phosphate adsorption capacity of the Fe–Cu binary oxide as a function of regeneration cycle.

phosphate adsorption. For an example, the phosphate adsorption rate reduced to 59% and 70%, respectively, when the concentration of silicate and fluoride increased from 0 to 10 mM. Silicate and phosphate are located in the adjacent position in the periodic table of the elements, and the molecular structure of the silicate ion is very similar to that of the phosphate ion. The obvious inhibition of silicate on phosphate adsorption may be due to the strong competition for the binding sites on the adsorbent between the phosphate and silicate. Fluoride has a strong electronegativity, and is easily combined with the protonated adsorbent surface. Therefore, the uptake of phosphate gradually decreased as its concentration increased.

### 3.6. Regeneration and reusability of the Fe–Cu binary oxide

To assess the reusability of the used Fe–Cu binary oxide, its regeneration using NaOH solution and re-adsorption were

investigated. These adsorption–regeneration cycles were carried out up to five times and the results were demonstrated in Fig. 6. The value of cycle 0 is the adsorption capacity of the fresh Fe–Cu binary oxide. The phosphate adsorption capacity of the Fe–Cu binary oxide slowly decreased with an increase in regeneration cycle. Whereas, this reduction was not so remarkable and about 69% of the original adsorption capacity was still achieved after 4 times regeneration. These indicate that the adsorption of phosphate on Fe–Cu binary oxide is relatively reversible and the spent Fe–Cu binary oxide could be regenerated via NaOH treatment.

### 3.7. Characterization before and after phosphate adsorption

The morphology and surface elements distribution of Fe–Cu binary oxide before and after phosphate adsorption were studied and the results were depicted in Fig. 7. The SEM images show that the Fe–Cu binary oxide was comprised of many aggregated nano-scale particles (Fig. 7A), which resulted in a rough surface. After phosphate adsorption, the morphology did not change significantly (Fig. 7C). The EDX analysis (Fig. 7B) revealed that Cu and Fe were evenly distributed on the surface and the Cu/Fe molar ratio on the surface was of 0.51, a little higher than that of bulk of  $0.491 \pm 0.012$ . In addition, the presence of sulfur element on the surface was observed. This might be ascribed to the residual sulfate since copper (II) sulfate pentahydrate was used to prepare the Fe–Cu binary oxide in this study. After phosphate adsorption, the sulfur peak disappeared and a new peak of phosphorus was observed (seen in Fig. 7D). This means that the phosphate was adsorbed on the surfaces of the binary oxide and at same time sulfate was completely replaced by the phosphate.

The FTIR spectra of samples before and after phosphate adsorption are shown in Fig. 8. For the sample of fresh Fe–Cu binary oxide sample, the peak at  $1632 \text{ cm}^{-1}$  was assigned to the deformation of water molecules, which indicated the presence of physisorbed water on the oxide. The peak at  $1364 \text{ cm}^{-1}$  could be ascribed to the adsorbed  $\text{CO}_3^{2-}$ , since the experiments were conducted in atmo-

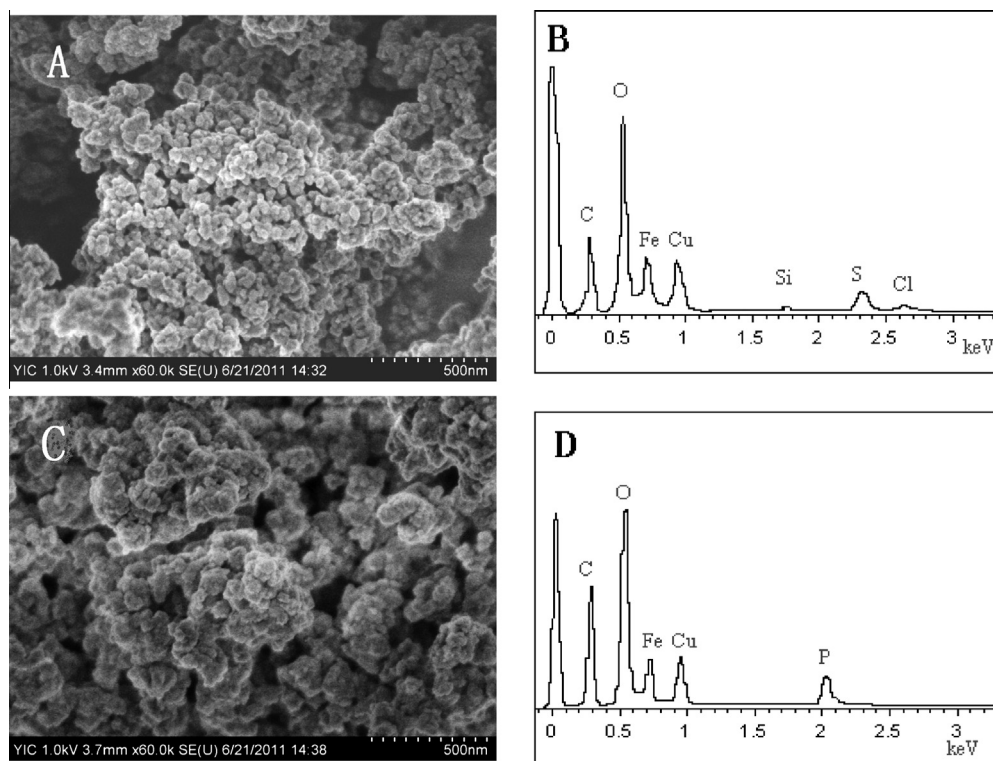


**Fig. 7.** SEM micrographs and EDX surface analysis of the Fe–Cu binary oxide with Cu/Fe molar ratio of 1:2 (A, C) before and (B, D) after phosphate adsorption.

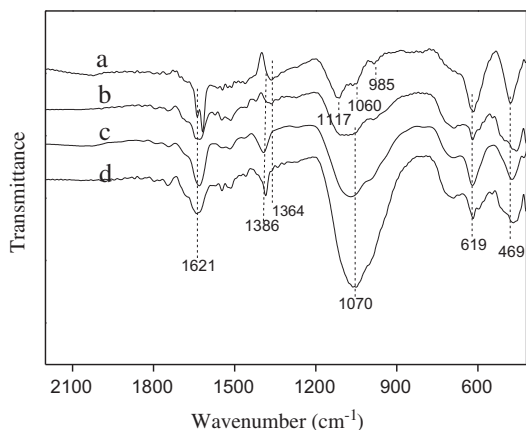


**Fig. 8.** FTIR spectra of Fe–Cu binary oxide. (a) Before and after treatment in aqueous solutions of three different phosphate concentrations, (b) 1 mg L<sup>-1</sup>, (c) 5 mg L<sup>-1</sup> and (d) 10 mg L<sup>-1</sup>.

sphere. Three peaks of 1117 cm<sup>-1</sup>, 1060 cm<sup>-1</sup> and 985 cm<sup>-1</sup> were attributed to the vibration of SO<sub>4</sub><sup>2-</sup> [34]. The peaks at 619 cm<sup>-1</sup> and 469 cm<sup>-1</sup> might be due to the overlap of Cu–O stretching [35] and the bulk OH deformations of ferrihydrite [36]. After reaction with phosphate, a new peak appeared at 1070 cm<sup>-1</sup>, which is broad and intensive and could be assigned to the asymmetry vibration of sorbed PO<sub>4</sub><sup>3-</sup> [34]. Meanwhile, the three peaks of SO<sub>4</sub><sup>2-</sup> vibration disappeared gradually with the increase in adsorbed phosphate and the intensity of surface OH vibration weakened. This suggests that the sulfate and hydroxyl groups on the surface of the oxide might be displaced by phosphates, which is consistent with the EDX results. In addition, the peak at 1364 cm<sup>-1</sup> was also disappeared gradually after phosphate adsorption and a new peak at 1386 cm<sup>-1</sup> was observed, which might be attributed to the shift of the vibration of sorbed CO<sub>3</sub><sup>2-</sup>.

#### 4. Conclusions

High performance Fe–Cu binary oxide sorbent was prepared using a facile coprecipitation method. The synthetic Fe–Cu binary oxides grains were aggregates formed by nanosized particles. The adsorption tests showed that the optimal Cu/Fe molar ratio was of 1:2 in term of adsorption capacity of phosphate. The maximal adsorption capacities for phosphate were 39.8 mg g<sup>-1</sup> at pH 5.0 ± 0.1 and 35.2 mg g<sup>-1</sup> at pH 7.0 ± 0.1, respectively, which outperformed most of reported sorbents. Thermodynamic and kinetic experiments demonstrated that the phosphate adsorption was a spontaneous, endothermic and chemically sorptive process. The results of ionic strength test along with FTIR analysis indicated that phosphate anions might form inner-sphere surface complexes at the water/oxide interface. The phosphate-loaded Fe–Cu binary oxide could be effectively regenerated by 0.5 mol L<sup>-1</sup> NaOH and re-used for the phosphate adsorption for several times. This adsorbent might be a promising adsorbent for the removal of phosphate from aqueous solutions.

#### Acknowledgements

The authors acknowledge financial support by National Natural Science Foundation of China (Grant No. 51178453). Xiwang Zhang specially thanks for the ARF Fellowship provided by Australia Research Council (DP110103533) and Larkins Fellowship by Monash University.

#### Appendix A. Supplementary material

Supplementary data associated with this article can be found, in the online version, at <http://dx.doi.org/10.1016/j.cej.2013.09.021>.

#### References

- [1] C. Barca, C. Gérente, D. Meyer, F. Chazarenc, Y. Andrès, Phosphate removal from synthetic and real wastewater using steel slags produced in Europe, *Water Res.* 46 (2012) 2376–2384.
- [2] C. Vohla, M. Köiv, H.J. Bavor, F. Chazarenc, Ü. Mander, Filter materials for phosphorus removal from wastewater in treatment wetlands – a review, *Ecol. Eng.* 37 (2011) 70–89.
- [3] S. Tanada, M. Kabayama, N. Kawasaki, T. Sakiyama, T. Nakamura, M. Araki, T. Tamura, Removal of phosphate by aluminum oxide hydroxide, *J. Colloid Interf. Sci.* 257 (2003) 135–140.
- [4] Y. Tang, E. Zong, H. Wan, Z. Xu, S. Zheng, D. Zhu, Zirconia functionalized SBA-15 as effective adsorbent for phosphate removal, *Micropor. Mesopor. Mat.* 155 (2012) 192–200.
- [5] D. Donnert, M. Salecker, Elimination of phosphorus from waste water by crystallization, *Environ. Technol.* 20 (1999) 735–742.
- [6] L.E. De-Bashan, Y. Bashan, Recent advances in removing phosphorus from wastewater and its future use as fertilizer (1997–2003), *Water Res.* 38 (2004) 4222–4246.
- [7] S.K. Kang, K.H. Choo, K.H. Lim, Use of iron oxide particles as adsorbents to enhance phosphorus removal from secondary wastewater effluent, *Separ. Sci. Technol.* 38 (2003) 3853–3874.
- [8] L.M. Blaney, S. Cinar, A.K. SenGupta, Hybrid anion exchanger for trace phosphate removal from water and wastewater, *Water Res.* 41 (2007) 1603–1613.
- [9] E.M. van Voorhuizen, A. Zwijnenburg, M. Wessling, Nutrient removal by NF and RO membranes in a decentralized sanitation system, *Water Res.* 39 (2005) 3657–3667.
- [10] D. Kurniadie, C. Kunze, Constructed wetlands to treat house wastewater in Bandung, Indonesia, *J. Appl. Bot. Angew. Bot.* 74 (2000) 87–91.
- [11] L.D. Hylander, A. Kietlinska, G. Renman, G. Simán, Phosphorus retention in filter materials for wastewater treatment and its subsequent suitability for plant production, *Bioresource Technol.* 97 (2006) 914–921.
- [12] E. Yildiz, Phosphate removal from water by fly ash using crossflow microfiltration, *Sep. Purif. Technol.* 35 (2004) 241–252.
- [13] B. Kostura, H. Kulveitova, J. Lesko, Blast furnace slags as sorbents of phosphate from water solutions, *Water Res.* 39 (2005) 1795–1802.
- [14] E. López, B. Soto, M. Arias, A. Núñez, D. Rubinos, M.T. Barral, Adsorbent properties of red mud and its use for wastewater treatment, *Water Res.* 32 (1998) 1314–1322.
- [15] M. Khadhraoui, T. Watanabe, M. Kuroda, The effect of the physical structure of a porous Ca-based sorbent on its phosphorus removal capacity, *Water Res.* 36 (2002) 3711–3718.
- [16] Y. Arai, D.L. Sparks, ATR–FTIR spectroscopic investigation on phosphate adsorption mechanisms at the ferrihydrite–water interface, *J. Colloid Interf. Sci.* 241 (2001) 317–326.
- [17] R. Chitrakar, S. Tezuka, A. Sonoda, K. Sakane, K. Ooi, T. Hirotsu, Phosphate adsorption on synthetic goethite and akaganeite, *J. Colloid Interf. Sci.* 298 (2006) 602–608.
- [18] O.R. Harvey, R.D. Rhue, Kinetics and energetics of phosphate sorption in a multi-component Al(III)–Fe(III) hydr(oxide) sorbent system, *J. Colloid Interf. Sci.* 322 (2008) 384–393.
- [19] G.S. Zhang, H.J. Liu, R.P. Liu, J.H. Qu, Removal of phosphate from water by a Fe–Mn binary oxide adsorbent, *J. Colloid Interf. Sci.* 335 (2009) 168–174.
- [20] F. Long, J.L. Gong, G.M. Zeng, L. Chen, X.Y. Wang, J.H. Deng, Q.Y. Niu, H.Y. Zhang, X.R. Zhang, Removal of phosphate from aqueous solution by magnetic Fe–Zr binary oxide, *Chem. Eng. J.* 171 (2011) 448–455.
- [21] A.F. Sousa, T.P. Braga, E.C. Gomes, A. Valentini, E. Longhinotti, Adsorption of phosphate using mesoporous spheres containing iron and aluminum oxide, *Chem. Eng. J.* 210 (2012) 143–149.
- [22] J.Y. Liu, Q. Zhou, J.H. Chen, L. Zhang, N. Chang, Phosphate adsorption on hydroxyl-iron-lanthanum doped activated carbon fiber, *Chem. Eng. J.* 215–216 (2013) 143–149.
- [23] J.B. Lü, H.J. Liu, R.P. Liu, X. Zhao, L.P. Sun, J.H. Qu, Adsorptive removal of phosphate by a nanostructured Fe–Al–Mn trimetal oxide adsorbent, *Powder Technol.* 233 (2013) 146–154.
- [24] G.S. Zhang, Z.M. Ren, X.W. Zhang, J. Chen, Nanostructured iron(III)–copper(II) binary oxide: a novel adsorbent for enhanced arsenic removal from aqueous solutions, *Water Res.* 47 (2013) 4022–4031.
- [25] J.C. Ryden, J.R. McLaughlin, J.K. Syers, Mechanisms of phosphate sorption by soils and hydrous ferric gel, *J. Soil Sci.* 28 (1977) 72–92.
- [26] M.B. McBride, A critique of diffuse double layer models applied to colloid and surface chemistry, *Clay Clay Miner.* 45 (1997) 598–608.
- [27] L. Zeng, X.M. Li, J.D. Liu, Adsorptive removal of phosphate from aqueous solutions using iron oxide tailings, *Water Res.* 38 (2004) 1318–1326.
- [28] H.L. Liu, X.F. Sun, C.Q. Yin, C. Hu, Removal of phosphate by mesoporous ZrO<sub>2</sub>, *J. Hazard. Mater.* 151 (2008) 616–622.
- [29] H. Li, J. Ru, W. Yin, X. Liu, J. Wang, W. Zhang, Removal of phosphate from polluted water by lanthanum doped vesuvianite, *J. Hazard. Mater.* 168 (2009) 326–330.

- [30] L.A. Rodrigues, M.L.C.P. da Silva, Thermodynamic and kinetic investigations of phosphate adsorption onto hydrous niobium oxide prepared by homogeneous solution method, *Desalination* 263 (2010) 29–35.
- [31] K.F. Lam, C.M. Fong, K.L. Yeung, Separation of precious metals using selective mesoporous adsorbents, *Gold Bull.* 40 (2007) 192–198.
- [32] K.F. Lam, X.Q. Chen, C.M. Fong, K.L. Yeung, Selective mesoporous adsorbents for  $\text{Ag}^+/\text{Cu}^{2+}$  separation, *Chem. Comm.* 17 (2008) 2034–2036.
- [33] X.Q. Chen, K.F. Lam, K.L. Yeung, Selective removal of chromium from different aqueous systems using magnetic MCM-41 nanosorbents, *Chem. Eng. J.* 172 (2011) 728–734.
- [34] G. Lefevre, In situ fourier-transform infrared spectroscopy studies of inorganic ions adsorption on metal oxides and hydroxides, *Adv. Colloid Interface* 107 (2004) 109–123.
- [35] K. Kliche, Z.V. Popovic, Far-infrared spectroscopic investigations on CuO, *Phys. Rev. B* 42 (1990) 10060–10066.
- [36] R.M. Cornell, U. Schwertmann, *The Iron Oxides: Structure, Properties, Reactions, Occurrences and Uses*, second ed., Wiley-VCH Verlag GmbH & Co. KGaA, Weinheim, 2003.